Inhibition of Cracking in Cu_6Sn_5 Intermetallic Compounds at Sn-Cu Lead-Free Solders and Cu Substrate Interfaces

K. Nogita[1], S. Suenaga[2], S. D. McDonald[1], H. Tsukamoto[1], J. Read[1] and T. Nishimura[2]
[1]Materials Engineering, The University of Queensland, St. Lucia, Brisbane QLD, 4072 Australia
[2]Nihon Superior Co. Ltd., NS Bldg., 1-16-15 Esaka-Cho, Suita City, Osaka, 564-0063 Japan

Abstract

The authors have successfully developed a method of limiting cracking in the Cu_6Sn_5 intermetallic compounds, which are formed at the interface between lead free solders and their Cu substrates. In this paper, it is shown that the level of cracking in the $(Cu,Ni)_6Sn_5$ reaction layer and the morphology of the intermetallics varies with the Ni content. To explore the mechanisms associated with the differences in joint integrity, detailed synchrotron X-ray powder diffraction (XRD) has been used with Rietveld analysis. The results show Ni stabilises a high temperature allotrope of the Cu_6Sn_5 phase avoiding stresses induced by a volumetric change that would otherwise occur on phase transformation .

Introduction

In the last few decades significant research has been directed at developing lead-free solders for the electronics industry[(1)]. One attractive group of lead-free solder alloys are those based on the Sn-Cu-Ni system which have found applications in wave, dip and iron soldering processes and are cheaper than most other candidate alloys due to the omission of expensive elements such as silver or rare earths[(2)]. The intermetallic Cu_6Sn_5 that forms between Sn-Cu lead-free solder alloys and Cu substrates influences the soldering process and the subsequent joint properties. Cu_6Sn_5 exists in two crystal structures with an allotropic transformation from monoclinic η'-Cu_6Sn_5 at temperatures lower than 186ºC to hexagonal η-Cu_6Sn_5. In conventional lead-free solder alloys the brittle Cu_6Sn_5 intermetallic is often associated with the presence of a large number of microcracks which may form in response to thermo-mechanically induced stresses associated with the phase transformation. The authors have successfully developed a method of limiting cracking in the Cu_6Sn_5 intermetallic compounds (IMC) by stabilising the high temperature hexagonal Cu_6Sn_5 phase with Ni additions[(3)]. The phase stability induced by Ni being present in the Cu_6Sn_5 phase and its possible implications are discussed with reference to the experimental results.

Experimental procedure

Cracking measurements

The nature of cracking in the reaction layer present in two types of samples, ball grid array (BGA) soldered and dipped Cu plate interfaces, has been investigated. Two compositions of lead-free solder were used, Sn-0.7wt%Cu (SC) and Sn-0.7wt%Cu-0.05wt%Ni (SCN). BGA type samples were obtained from 500µm diameter solder balls on organic solderability protection (OSP) Cu boards with a common reflow process. Figure 1 shows the reflow profile for the BGA process. This cycle was conducted twice for each BGA specimen.

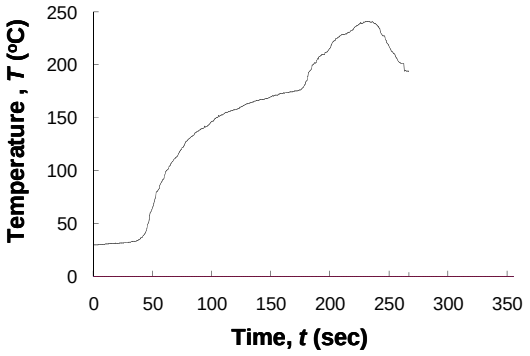

Figure 1. Temperature profile of a reflow process.

Dipped Cu type samples were obtained by dipping a Cu plate (C1220P), 10mm x 30mm x 0.3mm, with common flax into a molten solder held at in 250°C, 10 sec. Selected samples were subsequently annealed at 120°C for 1000 hours. All samples were embedded in resin and polished in cross-sectioned to observe the solder joint IMC using SEM/EDS. The microstructures of the samples were studied using SEM (JEOL JSM-6460LA, Japan) with 20kV in secondary image mode. The crack length and crack number of IMC was measured by digital imaging using commercial SEM image analysis software, JEOL AnalysisStation. The crack number and crack length were normalised by the total measured length of the solder joint, which was typically close to 300µm. EDS point elemental analysis of Sn, Cu and Ni in the IMC was conducted by the average of five measurements.

Phase stabilisation

To obtain Cu_6Sn_5 and $(Cu,Ni)_6Sn_5$ intermetallic particles for detailed experimentation, two types of samples (as cast sample 'A' and annealed 'B') were produced using a direct alloying method. High purity copper, tin (and nickel) ingots were placed in a clay-graphite crucible and heated to 700ºC in an electric resistance furnace under Ar gas flow. The melt was held at this temperature for a minimum of two hours. Using a stainless steel mould of 15mm diameter and 10mm height, approximately 15g of the alloy was cast from the melt and allowed to solidify while cooling in air. The solid sample was then annealed in a heat treatment furnace at 400 ºC for 528 hours and cooled to room temperature (designated series 'A') and selected samples were then subjected to a subsequent treatment of 180 ºC for 168 hours (designated series 'B'). Chemical analysis confirmed we obtained Cu_6Sn_5 and $Cu_{5.5}Ni_{0.5}Sn_5$ samples for both A and B series. The chemical analysis data of Cu_6Sn_5 and $(Cu,Ni)_6Sn_5$ are shown in Table 1.

Table 1. Chemical composition of XRD samples.

No.	Samples	Sample annealing conditions	Cmpostions (at%)		
			Cu	Ni	Sn
A1	Cu_6Sn_5	400°C 528hr	54.40	0.00	45.60
A2	$Cu_{5.5}Ni_{0.5}Sn_6$	400°C 528hr	50.12	4.58	45.30
B1	Cu_6Sn_5	400°C 528hr + 180°C 168hr	54.40	0.00	45.60
B2	$Cu_{5.5}Ni_{0.5}Sn_6$	400°C 528hr + 180°C 168hr	50.12	4.58	45.30

The sample was crushed in an agate mortar to obtain powder for the XRD experiments. XRD studies on the crystal structure and lattice parameters were carried out at the BL15 Kyushu synchrotron, SAGA-LS. The XRD spectra for the Rietveld structure refinement were obtained in the 2θ range of 20 to 75 degree after scanning from film exposed in a Debye-Scherrer type XRD machine. Rietveld analysis of the XRD signal peak intensities, peak profiles and peak positions were carried out using the RIETAN-2000[4] computer package. Standard silicon (NIST640C) powder, National Institute of Standards, was used for the calibration of the Rietveld analysis with identical experimental conditions used for the samples. For the refinement the parameters were optimized to minimize the residual ***R*wp**, ***R*p** and ***S*** factors[4]. Throughout the determination of the lattice parameters using structure refinement of the samples, V and W, which are both machine dependent parameters, and B, an isotropic displacement parameter, were fixed with the values obtained from the standard silicon powder as shown in Table2

Table 2 Refined Rietveld parameters for standard Si

Gaussian FWHM parameter, U	1.54E-03
Gaussian FWHM parameter, V	-8.67E-04
Gaussian FWHM parameter, W	3.31E-04
Scherrer coefficient for Gaussian broadening, P	0
Lorentzian Scherrer broadening, X	1.77E-02
Anisotropic Scherrer broadening, Xe	0
Strain broadening, Y	7.69E-03
Anisotropic strain broadening, Ye	0
Preferred-orientation parameter, r	1
Lattice parameter, a	5.43119
Lattice parameter, b	5.43119
Lattice parameter, c	5.43119
Lattice parameter, α	90
Lattice parameter, β	90
Lattice parameter, γ	90
Overall isotropic displacement parameter, Q	0
Silicon atom Occupation factor, g	1
Fractional coordinate, x	0
Fractional coordinate, y	0
Fractional coordinate, z	0
Isotropic displacement parameter, B	0.58
R wp	12.74
R p	8.00
R b	2.85
S	1.09

Results and discussion

Observation and quantification of cracking at the soldered interface

Figure 2 to 4 show SEM micrographs of cross-sectioned BGA, dipped Cu type samples and dipped Cu samples with subsequent 120°C annealing of (a) SC and (b) SCN, respectively. Visible cracks can be seen in the intermetallic

compound (IMC) layer between the solder alloy and the Cu substrate on (a) SC alloy but not or few in (b) SCN alloys where Ni is present.

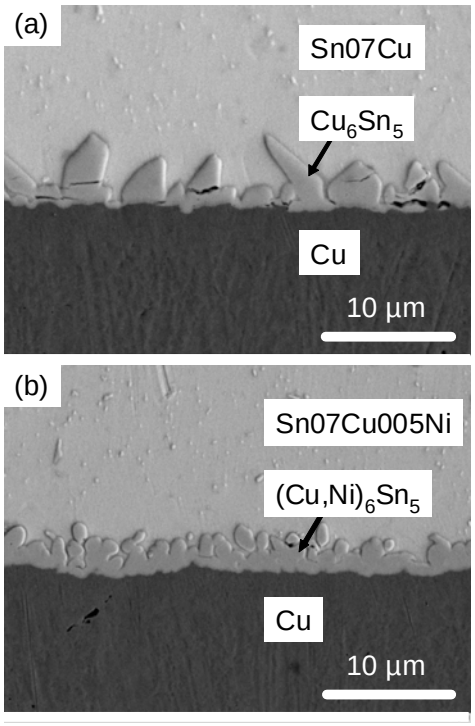

Figure 2. Cross-sectioned SEM image of BGA solder structures of (a) SC and (b) SCN.

Table 3 Chemical compositions of IMC

Samples	Cu (at%)	Ni (at%)	Sn (at%)
BGA-SC	58	0	42
BGA-SCN	51	5	44
Dip-SC	57	0	43
Dip-SCN	52	5	43

It is noted that all cracks formed in IMC are near parallel to the Cu substrate, but none are perpendicular or present in other directions. This tendency may be due to the growth direction of IMC as determined by the interface crystallography or thermal conditions combined with a preferred habit plain for cracking, or otherwise related to the direction of stresses during thermal expansion . Further investigations on the crack orientation are required. The IMC present in this layer is commonly known to be Cu_6Sn_5 and it is apparent significantly fewer cracks are present in the Cu_6Sn_5 layer when Ni is present in the Sn-0.7Cu solder. According to the literature a Cu_3Sn layer may be present between the Cu substrate and the Cu_6Sn_5 IMC in all samples[5], however, this must be very thin and could not recognized in the current study at the limits of SEM magnification. Table 3 shows EDS elemental analysis results (fine average point) of the IMC layer. The chemical composition of the IMCs are Cu_6Sn_5 or $(Cu,Ni)_6Sn_5$. It is obvious that the IMC in SCN samples of BGA and dipped Cu contain about 5at% Ni to form $(Cu,Ni)_6Sn_5$. Since the only source of Ni is in the solder for SCN samples, it is expected that the 5at% Ni migrate from the solder during growth of the IMC layer.

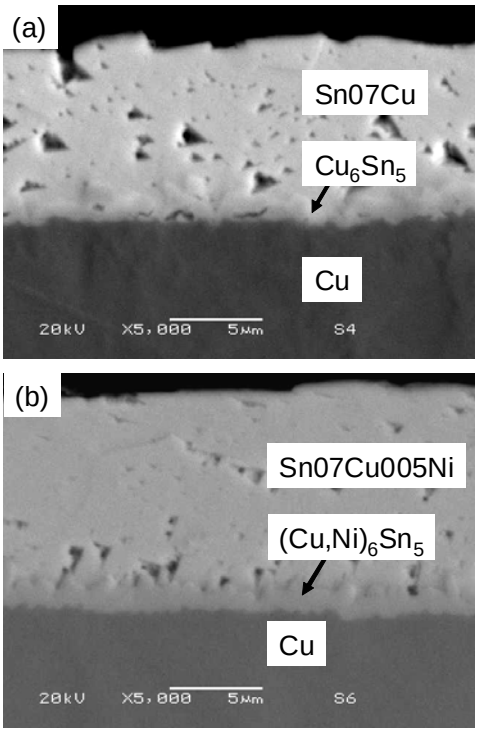

Figure 3. Cross-sectioned SEM image of dipped Cu sample of (a) SC and (b) SCN.

Figure 5 to 7 indicate the normalized crack length and crack number in IMCs of BGA, dipped Cu and dipped Cu with subsequent annealing samples, respectively. The IMC layers in SCN solders, which contain around 5 at% Ni, experience less cracking than those without Ni in all solder conditions and there are no cracks present in dipped Cu samples of SCN solder. Therefore, by including Ni in the solder cracking can be inhibited at the solder joint by in the IMC layer. In the next section, we demonstrate the mechanism of crack inhabitation is likely to be related to phase stabilisation by using synchrotron powder XRD for Cu_6Sn_5 and $(Cu,Ni)_6Sn_5$ with 5 at%Ni samples.

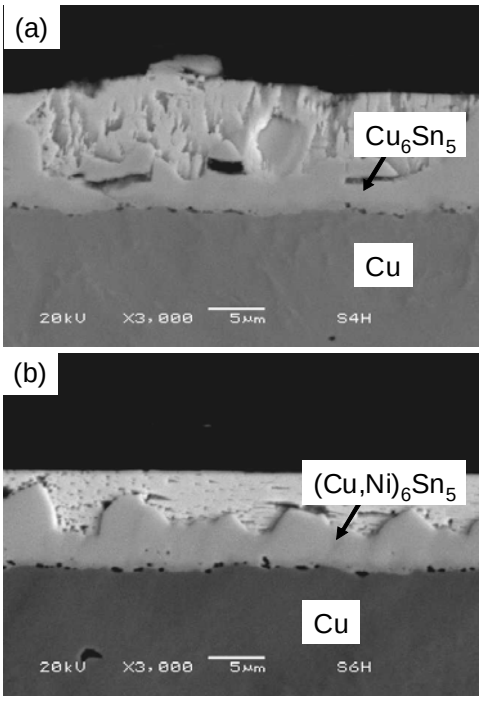

Figure 4. Cross-sectioned SEM image of dipped Cu with 120C annealed sample of (a) SC and (b) SCN.

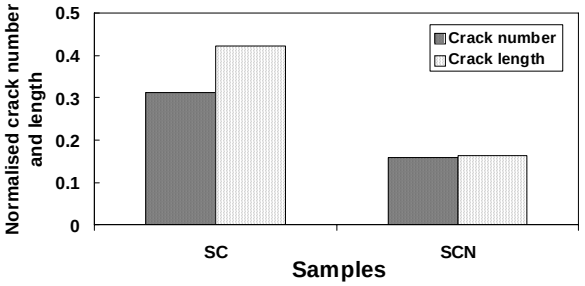

Figure 5 Normalised crack length and number in IMC of BGA

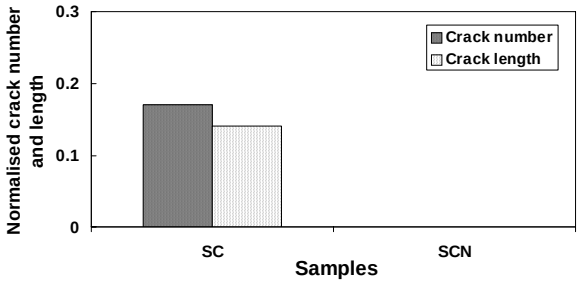

Figure 6 Normalised crack length and number in IMC of dipped Cu sample

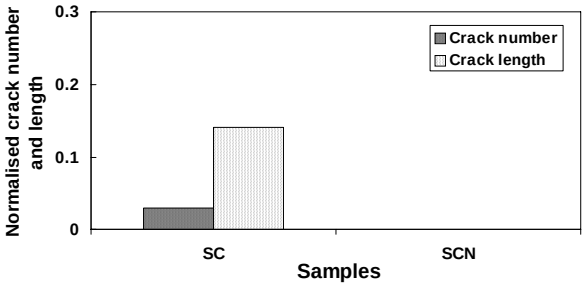

Figure 7 Normalised crack length and number in IMC of dipped Cu sample with annealing.

Crystallography and phase stability of IMCs

From the reported phase diagram[5], Cu_6Sn_5 exists in two crystal structures with an allotropic transformation from monoclinic η'-Cu_6Sn_5 at temperatures lower than 186ºC to hexagonal η-Cu_6Sn_5. Ambient temperature theoretical densities of monoclinic and hexagonal are evaluated as 8.270 g/cm^3 and 8.448 g/cm^3, respectively[6]. This means if the IMC makes a phase transformation from the 'quenched' hexagonal phase to monoclinic phase during operation, there will theoretically be a 2.15% volume expansion, which would conceivably be accompanied by significant stress in the IMC layer. We assumed the lower cracking in the SCN compositions are due to the avoidance of the phase transformation and the associated volume change when the hexagonal phase is stabilized by Ni. Table 4 show fractional coordinates for the Rietveld analysis of RIETAN-2000[4] of (a) hexagonal η-Cu_6Sn_5 ($P6_3/mmc$) and (b) monoclinic η'-Cu_6Sn_5 (C2/c). There are very small differences in of the X-ray diffraction peaks between the two except for the strong peak height ratio and the presence of several relatively weak peaks in the 2 theta range of 25-50°[6]. Therefore, strong synchrotron X-ray was required to distinguish between the two.

Table 4. Unit cell-external parameters of (a) hexagonal η-Cu_6Sn_5 ($P6_3/mmc$) and (b) monoclinic η'-Cu_6Sn_5 (C2/c).

(a) $P6_3/mmc$

Atom	Site	Occ	x	y	z
Sn1	2(c)	1	0.333	0.667	0.250
Cu1	2(a)	1	0.000	0.000	0.000
Cu2	2(d)	0.2	0.333	0.667	0.750

(b) C2/c

Atom	Site	Occ	x	y	z
Cu1	8(f)	1	0.101	0.473	0.202
Cu2	8(f)	1	0.306	0.504	0.610
Cu3	4(a)	1	0.000	0.000	0.000
Cu4	4(e)	1	0.000	0.160	0.250
Sn1	8(f)	1	0.391	0.162	0.529
Sn2	8(f)	1	0.285	0.655	0.358
Sn3	4(e)	1	0.000	0.799	0.250

To compare the effects of Ni on the crystallography, the XRD pattern obtained from A1 (Cu_6Sn_5) and A2 ($Cu_{5.5}Ni_{0.5}Sn_5$), and Bl (Cu_6Sn_5) and B2 ($Cu_{5.5}Ni_{0.5}Sn_5$), samples are shown in Figure 8a and 8b. XRD peaks clearly shows a hexagonal Cu_6Sn_5 structure in all Ni containing samples present as $Cu_{5.5}Ni_{0.5}Sn_5$ (A2 and B2) but no monoclinic phase was detected, while all samples without Ni (A1 and B1) clearly indicate small peaks, which are expected from the monoclinic phase. The doted area of the figures between 30 to 45 º in 2θ is magnified, and small extra peaks which are not present in hexagonal diffractions are indicated with arrows. Intensities of weak monoclinic peaks are higher in B1 sample than A1 sample. This suggests sample A1 (non-annealed at 180°C sample) may contain a mixture of hexagonal and monoclinic as a result of being 'quenched' from 400°C. XRD analysis of monoclinic Cu_6Sn_5 without Ni present has been reported by Ghosh and Asta[6] using samples annealed at 150°C for 80 days. They reported several relatively weak peaks in the 2θ range of 25 - 50º clearly in monoclinic Cu_6Sn_5, which could not be found in the present $(Cu,Ni)_6Sn_5$ samples both with and without annealing. It is concluded that in the current study for this condition, around 5 at% of Ni in Cu_6Sn_5 stabilised the high temperature hexagonal phase. Furthermore, cracking of IMCs in SC samples shown in Figures 2a, 3a and 4a are expecting to result from phase transformation from hexagonal to monoclinic during cooling. Also, importantly, it was noted that the degree of cracking in the SC samples and the potential for more cracking during loading is likely to depend on the cooling rate related to phase transformation kinetics and temperature, since it is expected that the transformation is incompleted.

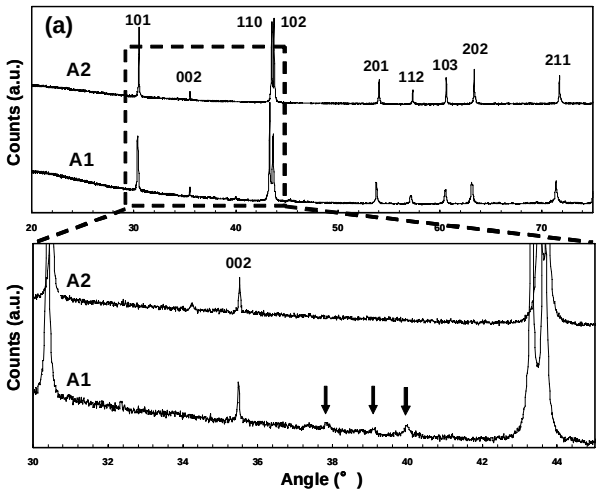

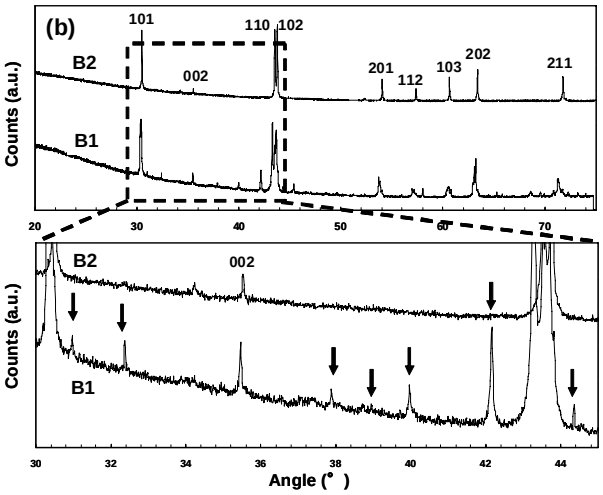

Figure 8. XRD peaks of (a) A1 (Cu_6Sn_5) and A2 ($Cu_{5.5}Ni_{0.5}Sn_5$), and (b) B1 (Cu_6Sn_5) and B2 ($Cu_{5.5}Ni_{0.5}Sn_5$). Doted area between 30-45° in 2θ is magnified.

Table 5 shows the Rietveld analysis results of annealed Cu_6Sn_5 (B1) and $Cu_{5.5}Ni_{0.5}Sn_5$ (B2) samples based on hexagonal ($P6_3/mmc$) and monoclinic (C2/c) structure settings. Comparing the refinement parameters of ***R*wp**, ***R*p** and ***S***[4] of hexagonal and monoclinic settings (lower values for these parameters indicate a better match) the Cu_6Sn_5 sample (B1) is a better fit for the monoclinic (C2/c) phase than for the hexagonal phase ($P6_3/mmc$). It is expected that not only small monoclinic peaks but the intensity ratio of each strong peak are a better fit for monoclinic refractions than that of hexagonal. In contrast the $Cu_{5.5}Ni_{0.5}Sn_5$ sample (B2) is a better fit for the hexagonal phase. In conclusion, it is clear that the Cu_6Sn_5 sample with annealing at 180°, which is just below the reported phase transformation temperature, shows a monoclinic structure but does not show any of the hexagonal high temperature phase. This result is in agreement with previously reported results[3].

Table 5. Rietveld analysis results of annealed Cu_6Sn_5 (B1) and $Cu_{5.5}Ni_{0.5}Sn_5$ (B2)

Samples	Crystallographic setting	*R* wp	*R* p	S
B1	Monoclinic	6.81	4.42	2.95
B1	Hexagonal	7.35	4.63	3.18
B2	Monoclinic	7.74	4.81	2.45
B2	Hexagonal	5.42	3.78	1.72

Table 6. Lattice parameters of annealed Cu_6Sn_5 (B1) and $Cu_{5.5}Ni_{0.5}Sn_5$ (B2)

Samples	Lattice parameters (Å)			
	a	a(STD)	c	c(STD)
B1	4.223	0.002	5.113	0.002
B2	4.197	0.002	5.103	0.001

To analyse how lattice parameters change with Ni content, we used the hexagonal crystallographic data of $P6_3/mmc$ for all samples. As shown in Table 6, both 'a' axis and 'c' axis decrease their lattice parameters with Ni contents, however, the 'a' axis displays a larger decrease than that of the 'c' axis. Recently, Yu et. al.[7] reported the structural and electrical properties of $Cu_{6-x}Ni_xSn_5$ (with x=0, 1,2) from first-principles calculations. Assuming that the low temperature phase was monoclinic η'-Cu_6Sn_5, they concluded that, as the Cu sites are periodically substituted by Ni on Cu2 or 8f sites, the volume of the unit cells shrunk and the distance between atoms shortened. Based on energy and density of states calculations they demonstrated that stoichiometric ternary $Cu_{6-x}Ni_xSn_5$ compounds are more stable than Cu_6Sn_5 and that $Cu_4Ni_2Sn_5$ is the most stable phase. The measured compositions of IMCs in Table 1 of this study show that the IMCs are close to $Cu_{5.5}Ni_{0.5}Sn_5$. Present results of XRD show a systematic 'shrinking' of the lattice parameter (or volume per unit cell), must be due to Ni atoms in the lattice.

Conclusions

A method of limiting cracking in the Cu_6Sn_5 intermetallic compounds found at the interface of lead free solder alloys and their substrates has been successfully developed by adding small amount of Ni to a Sn-Cu lead-free solder. The intermetallic layers in Sn-Cu-Ni solders experience less cracking than those without Ni present. Synchrotron XRD was used to show that the stabilisation of the hexagonal $(Cu,Ni)_6Sn_5$ occurs in when Ni-containing solder alloys are used. This phase stabilization may prevent volume changes that could contribute to the cracking process in the IMC layer in Ni-free alloys where the hexagonal-monoclinic transformation occurs at approximately 186 ºC.

Acknowledgment

This research had been conducted under an international cooperative research program between the University of Queensland, Australia and Nihon Superior Company, Japan. XRD experiments were performed at the BL15 in the SAGA Light Source (SAGA-LS) under the Nanotechnology Support Project of the Ministry of Education, Culture, Sports, Science and Technology, Japan (project ID: 080625N). The author thanks Dr. T. Yamashita at Mesaplexx Pty. Ltd. for Rietveld analysis and Drs R. Ohtani and K. Sumitani of SAGA-LS for valuable discussions and XRD experiments.

References

(1) Y. Li, K.-s. Moon, and C.P. Wong, "Electronics without lead" Science, vol.308, pp. 1419-1420, 2005.

(2) K. Nogita, et al., "Microstructure control in Sn-0.7mass%Cu alloys" Materials Transactions, vol.46, pp. 2419-2425, 2005.

(3) K. Nogita and T. Nishimura, "Nickel-stabilized hexagonal $(Cu, Ni)_6Sn_5$ in Sn–Cu–Ni lead-free solder alloys " Scripta Materialia, vol.59, pp. 191-194, 2008.

(4) F. Izumi and T. Ikeda, "A Rietveld-analysis program RIETAN-98 and its applications to zeolites" Materials Science Forum, vol.321-324, pp. 198-205, 2000.

(5) T. Laurila, V. Vuorinen, and J.K. Kivilahti, "Interfacial reactions between lead-free solders and common base materials" Materials Science and Engineering R, vol.49, pp. 1-60, 2005.

(6) G. Ghosh and M. Asta, "Phase stability, phase transformations, and elastic properties of Cu_6Sn_5: Ab initio calculations and experimental results" Journal of Materials Research, vol.20, pp. 3102-3117, 2005.

(7) C. Yu, et al., "First-principles investigation of the structural and electronic properties of $Cu_{6-x}Ni_xSn_5$ (x = 0, 1, 2) intermetallic compounds" Intermetallics, vol.15, pp. 1471-1478, 2007.